DEPARTMENT OF MATHEMATICS

Steady Flow in Channels with Decreasing Discharge: Theory and Computation.

by

D. Porter & A. Priestley

Numerical Analysis Report **9/92**

UNIVERSITY OF READING

Steady Flow in Channels with Decreasing Discharge: Theory and Computation.*

D. Porter & A. Priestley

Institute for Computational Fluid Dynamics,

Department of Mathematics,

University of Reading,

Whiteknights,

Reading,

United Kingdom.

October 7, 1992

*The work reported here forms part of the research programme of the Reading/Oxford Institute for Computational Fluid Dynamics.

0 Abstract

A steady channel flow is considered in which the fluid discharges from the channel at a rate dependent on its local depth and attains a prescribed state at the downstream end. Practical examples of such flows are provided by side-weirs and racks. Using the standard assumptions of hydraulic theory, overall properties of the flow are determined for a general discharge law. The additional quantitative detail available for a specific law, including a classification diagram which summarises the available flow types, is illustrated for the side-weir. The analysis is supplemented by a robust, and accurate, numerical method capable of performing the required backwater calculations for sub-, super- and transcritical flows. The numerical technique can extend the applications to include tapering channels and friction effects.

1 Introduction

The purpose of this paper is to describe an investigation of the steady flow of water in straight channels with a decreasing discharge. The situation envisaged can be achieved in practice, for example, by a side-weir, consisting of a low sill on one or both sides of the channel, or a grating or rack in the channel bed. Background information regarding these particular practical applications can be found in Chow [2] and Henderson [4].

Using the standard assumptions of channel flow and measuring the coordinate x along the channel, the rate of change of the water depth $y(x)$ satisfies

$$y\prime = \frac{S_0 - S_f - \alpha\tilde{Q}\tilde{Q}\prime/gA^2 + \alpha F^2 y B\prime/B}{(1-\alpha F^2)}. \tag{1.1}$$

Chow [2] gives this formula in the case where the breadth, $B(x)$, of the channel is a constant. Here S_0 and S_f respectively denote the bed-slope and the friction slope and $A = By$ is the cross-sectional wetted area; g is the acceleration due to gravity. We shall assume that flow takes place in the positive x direction, so that the components of velocity and massflow in that direction, u and $\tilde{Q} = uA$ respectively, take non-negative values. The Froude number $F = u/\sqrt{gy}$ in this case.

The parameter $\alpha > 0$ is used to model energy loss. For the purposes of analysing the flow we shall take $\alpha = 1$, but this does not represent a restriction on the theoretical approach or on the numerical method to be presented later. The friction slope is typified by Manning's formula,

$$S_f = A^{-10/3}\tilde{Q}^2 n^2 (2y + B)^{4/3}, \tag{1.2}$$

where n is a given constant. It is generally considered that friction is not too important in the present context because of the short scale of the channels. Accordingly, we shall set $S_f = 0$ when establishing the theoretical properties of the flow, but the numerical scheme can easily accomodate (1.2), or indeed any other friction law that may be preferred by hydraulic engineers in a practical situation.

The principle assumptions leading to (1.1) are that the pressure is hydrostatic, so that the provisions of shallow water theory apply, and that the channel breadth is slowly-varying, allowing the quasi-one-dimensional model to be used. These assumptions are not invalidated by the discharge (see, for example, Chow [2]). We suppose that the discharge law has the form

$$\tilde{Q}\prime = -f(y - s), \tag{1.3}$$

where $s = s(x)$ is some assigned control level and

$$f(y) = H(y)g(y), \tag{1.4}$$

where $g(y)$ is a non-negative increasing function and $H(y)$ is the Heaviside function defined by

$$H(y) = 0 \quad (y < 0)$$

$$= 1 \quad (y > 0).$$

The discharge laws for the two applications alluded to earlier may be found in Chow [2]. For a side-weir,

$$g(y) = cy\sqrt{2gy}, \tag{1.5}$$

$c > 0$ being the weir-coefficient; in this case s represents the height of the sill above the bed-level. For discharge through a rack, the standard laws have $s = 0$ and

$$g(y) = \epsilon cB\sqrt{2gy + u^2}, \tag{1.6}$$

if the flow through the rack is vertical and

$$g(y) = \epsilon cB\sqrt{2gy}, \tag{1.7}$$

if the discharge is inclined to the rack. In both these expressions c is the coefficient of discharge through the openings of the rack and ϵ is the ratio of the opening area to the total area of the rack. The vertical discharge law, (1.6), assumes $\alpha = 1$ and a horizontal channel.

Note that (1.1) can be written as

$$\left(y + \tilde{Q}^2/2gA^2\right)\prime = S_0 - S_f, \tag{1.8}$$

having set $\alpha = 1$. It is convenient, for the theoretical discussion, to replace $\tilde{Q}$ by the massflow per unit breadth of the channel, $Q = \tilde{Q}/B = uy$ and write (1.8) as

$$\left(y + u^2/2g\right)' = -b', \tag{1.9}$$

in the absence of friction. Here $b(x)$ is the elevation of the bed above some datum level so that $b' = -S_o$. The discharge equation (1.3) is correspondingly altered to $(BQ)' = -f(y - s)$ which we may use in the form

$$Q' = -f(y - s), \tag{1.10}$$

for channels of constant breadth, with the parameter c in each of (1.5), (1.6) and (1.7) reinterpreted as the discharge coefficient per unit breadth of the channel.

The theoretical investigation will be based on the shallow water momentum and mass balance equations (1.9) and (1.10) and their counterparts at a stationary hydraulic jump, namely

$$[u^2 y + \frac{1}{2} g y^2] = 0, \quad [uy] = 0. \tag{1.11}$$

These jump conditions are derived in, for example, Stoker [9], the notation being that $[\phi] = \phi_+ - \phi_-$, where ϕ_+ is the value of ϕ on the downstream side of the jump and ϕ_- is its upstream value. Stoker also establishes that

$$[y + u^2/2g] < 0, \tag{1.12}$$

expressing energy loss across the jump.

The discharging channel is assumed to occupy the interval $[x_i, x_o]$, the practical applications requiring that the flow is specified at the outlet position

x_o. A so-called backwater analysis of the governing equations is therefore required to establish, for instance, whether a flow is possible for given outlet conditions and an assigned inlet position x_i.

In section 2 we shall determine the overall characteristics of discharge flows in general, irrespective of the particular form of the discharge law. This generality is achieved, in effect, by regarding Q as an independent variable. Many of the known properties of side-weir flows are deduced here for a general discharge law, without recourse to detailed analysis involving a specific law. To obtain more specific results for a particular type of discharge we need to determine the mapping between Q and x, and illustrate this in section 3 with particular reference to the side-weir case for which we give a classification diagram showing the type of flow for given outlet conditions and channel length.

Finally, in section 4, a novel numerical approach, based on the trapezium rule, will be presented that can perform approximate backwater analyses for not just subcritical flow, as is usually the case, but also for supercritical flow. Physical solutions to transcritical flows can also be found as the method does not blow up as the solution passes through the critical point $F = 1$. The method will be shown to be second order accurate for smooth flows. This numerical integration approach can clearly apply in situations where the analytic methods are not tractable and can be used to both confirm and extend the derived analytic properties.

2 Properties of Flows with Decreasing Discharges

To obtain a qualitative description of general flows with decreasing discharges, it is convenient to introduce two new variables and work with

$$Q = uy, \quad P = u^2 y + \frac{1}{2} g y^2, \quad e = y + \frac{u^2}{2g}, \tag{2.1}$$

which are the massflow (per unit channel breadth), the specific momentum and the specific energy, respectively. The quantity P has the values of $p + Qu$, where $p = \frac{1}{2} g y^2$ is the vertically averaged hydrostatic pressure, and is also referred to as the flow stress (in, for example, Sewell and Porter [8]). The energy $h = ge$ can be called the total enthalpy, by virtue of the gas dynamics–shallow water theory analogy. We note that Q, P and e take non-negative values because $y \geq 0$ on physical grounds and $u \geq 0$ by assumption.

The variables Q, P and e provide a concise description of the dynamical equations, for (1.9) and (1.10) can be written as

$$e_t = -b_t, \qquad Q_t = -f(y - s), \tag{2.2}$$

and at a stationary hydraulic jump, we see from (1.11) and (1.12) that the appropriate conditions are

$$[Q] = 0, \quad [P] = 0, \quad [e] < 0. \tag{2.3}$$

Further, boundary conditions may be provided directly in terms of the massflow and specific energy or may be converted into these quantities if given in terms

of u and y. It should be noted that, for the purpose of this discussion, we are considering only channels of constant breadth.

An informative geometrical description of the flows governed by (2.2) and (2.3) can be derived by observing that the equations (2.1) define a surface in Q, P, e space obtained by regarding u and y as parameters. Corresponding to any point in a steady shallow flow, specified by particular values of u and y, there is a point on the surface so defined. A complete flow can therefore be represented by a track on this surface, traced out as u and y vary through the flow from inlet to outlet, or from outlet to inlet in the case of a backwater analysis. At a hydraulic jump the track will transfer from one point on the surface to another point on the surface, in accordance with (2.3).

This notion, of representing flows by tracks on what may be called constitutive surfaces was introduced by Sewell and Porter [8] for gas dynamics and shallow water theory. In this previous work a more general setting is envisaged than we need here: the flows may be unsteady and rotational and the motion of individual fluid particles can then be represented by tracks. Other constitutive surfaces spanned by different variables can be considered, but these are ultimately less useful than the surface generated by (2.1), because of the simplicity of the dynamical conditions when expressed in terms of the variables Q, P and e.

The shape of the surface spanned by Q, P and $h = ge$ has been determined (Sewell and Porter [8]) and only the salient features need be given

here; the scaling introduced by using e in place of h is easy to accommodate. The surface has the swallowtail shape familiar in catastrophe theory and Figure 1 displays part of the surface in the octant of physical interest. The lower part of the surface corresponds to supercritical flows ($F > 1$), the upper part to subcritical flows ($F < 1$) and the two parts of the surface join at a cusped edge where $F = 1$. Expressing the surface as $P = P(Q, e)$, we easily find that

$$\frac{\partial P}{\partial Q} = u, \qquad \frac{\partial P}{\partial e} = gy, \tag{2.4}$$

and the second of these allows us to replace y in (2.2) by $g^{-1}\partial P/\partial e$ completing the task of expressing the dynamical equations in terms of the three new variables.

The arrow superposed on Figure 1 is the geometrical representation of the jump conditions (2.3). It is parallel to the e-axis and its direction indicates the sense of the jump as imposed by the inequality in (2.3), which must, of course, transform a supercritical flow into a subcritical flow.

To add some more detail to the swallowtail surface it turns out to be sufficient to consider its cross-section $e =$ constant, which is given in Figure 2 for $e = 1$. The value of Q corresponding to the critical value $F = 1$ is

$$Q_c(e) = g^{\frac{1}{2}}\,(2e/3)^{\frac{3}{2}}\,, \tag{2.5}$$

the greatest value of the massflow possible at a fixed specific energy level. The corresponding value of P is $P_c(e) = 2ge^2/3$ and the slope of both branches of the curve at the cusp is the critical speed $u_c(e) = (2ge/3)^{1/2}$. By virtue of (2.4),

this slope is the minimum speed of the supercritical flow and the maximum speed of the subcritical flow, with specific energy e. It follows that the critical depth $y_c(e) = Q_c(e)/u_c(e) = 2e/3$ is the maximum depth of the supercritical flow and the minimum depth of the subcritical flow. The slopes of the upper and lower branches at $Q = 0$ are 0 and $(2ge)^{1/2}$ respectively; these are the minimum and maximum values of u, at the given e.

We now superimpose the dynamical equations on these geometrical properties to determine a qualitative description of the flow. The outlet position x_o can be regarded as fixed and the values $Q_o = Q(x_o)$ and $e_o = e(x_o)$ as assigned. The first objective is to determine whether a flow can exist for the given values of Q_o and e_o and a chosen inlet position x_i. If a flow is possible, Q, e, u and y are to be calculated for $x_i \leq x \leq x_o$; of particular interest are the inlet values $Q_i = Q(x_i)$, $e_i = e(x_i)$, $u_i = u(x_i)$ and $y_i = y(x_i)$. For the present we shall tacitly assume that this calculation can be carried out, postponing details until the following sections.

For a flow to be possible, it is necessary that $Q_o \leq Q_c(e_o)$, that is,

$$Q_o \leq g^{\frac{1}{2}} (2e_o/3)^{\frac{3}{2}},$$

and we shall assume that this condition is met. It is automatically satisfied if u_o and y_o are given and (2.1) is used to find Q_o and e_o.

From (2.2) and the assumed properties of f we deduce that Q is a non-increasing function of x. More specifically, Q decreases as x increases if the

free surface is above the given control level s and Q is constant if the free surface is below this level. In both cases Q_o is the minimum value which Q can take in the flow.

2.1 Horizontal bed

To fix ideas, suppose that the channel is horizontal; non-zero bed slopes can easily be accommodated later, as we shall indicate. In this case, e = constant, wherever (2.2) applies. Assuming first that a continuous flow exists for $x_i \leq x \leq x_o$, then

$$e = e_o \quad (x_i \leq x \leq x_o)$$

and, in particular, $e_i = e_o$. This focuses attention on the swallowtail cross-section, typified by Figure 2, but with $e = e_o$.

If we further suppose that s is a constant we need only consider situations in which $y_o > s$, for otherwise there is a trivial solution consisting of a uniform flow at, or below, the control level. Therefore, Q decreases through at least part of the flow and $Q_i > Q_o$. For the assumed continuous flow to be possible it is necessary that

$$Q_i \leq Q_c(e_o). \tag{2.6}$$

Figure 3 illustrates (for $e_o = 1$) the two possible solution tracks for a continuous flow, assuming (2.6) is met; the sense of the arrows is from inlet to outlet. If Q_o and e_o are given at outlet, both sub- and supercritical flows are available.

Assigning u_o and/or y_o selects between these flows.

Note that, by (2.4), the change in u in the flow is equal to the change in slope of the solution track. Therefore, for $F_o < 1$ ($F_o > 1$), u decreases (increases) as the flow proceeds down the channel. Since e is constant, (2.1) shows that y increases (decreases) through the flow. It follows that, for a supercritical flow, $y \geq y_o > s$ ($x_i \leq x \leq x_o$) and the channel is therefore terminated by (2.6).

In the case of a subcritical flow, however, $y \leq y_o$ ($x_i \leq x \leq x_o$), introducing the possibility that the flow level coincides with the control level s at some point $x_s \in (x_i, x_o)$. The solution may then consist of a uniform critical or subcritical flow in which $y = s$, for $x_i \leq x \leq x_s$, joining at $x = x_s$ the subcritical flow which raises the fluid to the required depth at outlet. This two part solution is acceptable for present purposes if all of the variables are continuous and have continuous derivatives at $x = x_s$. Whether the required continuity is available depends upon the discharge law.

The subcritical case is not difficult to quantify. Note first that $e_o > y \geq s$, by assumption, and that the minimum depth is $y_c(e_o) = 2e_o/3$. Therefore, if $s < 2e_o/3$, $y > s$ throughout the flow. If, however, $2e_o/3 < s$, $y = s$ will be attained if the massflow is equal to $Q_s(e_o) = s\sqrt{2g(e_o - s)}$ within the flow. With $s = 2e_o/3$, $y = s$ occurs at critical flow and $Q_s(e_o) = Q_c(e_o)$.

We now see that the condition (2.6) is both necessary and sufficient

for the continuous flow to exist in the two cases specified by the outlet conditions

$$\left.\begin{array}{ll} \text{(a)} & F_o > 1, \\ \text{(b)} & F_o < 1, \quad e_o > 3s/2 \end{array}\right\}. \tag{2.7}$$

As $Q(x)$ is completely determined by (2.2) and the outlet conditions, assumed fixed, (2.6) is effectively a restriction on the channel length in these two cases. Flow is possible for all channels up to a maximum length $x_o - x_i$ determined by $Q_i = Q_c(e_o)$, and is not possible for longer channels.

For subcritical flows with $s < e_o \leq 3s/2$, (2.6) is automatically satisfied and and does not act as a restriction on channel length. If the inlet position x_i is such that $Q_i < Q_s(e_o)$, the continuous flow exists with the water level wholly above the level s. For a sufficiently long channel the massflow Q_s will be attained in the channel and the two part solution is possible with $Q_i = Q_s$; the length of the channel over which the uniform flow takes place is clearly a matter of indifference. If the two part solution is not acceptable, the channel length is limited by the condition $Q_i = Q_s$.

Suppose now that, for given outlet conditions in the categories (2.7), no continuous flow is possible. As we have indicated, this will be the case for all channels whose length exceeds a certain value. A discontinuous flow may nevertheless exist in which two continuous flows are connected across a hydraulic jump. Since the flow crossing a jump is necessarily subcritical on the downstream side, there can be no such solution in the case (2.7)(a) and our attention is restricted to (2.7)(b).

In the situation envisaged, (2.2) now implies that

$$\left.\begin{aligned} e &= e_o \quad (x_j < x \leq x_o), \\ &= e_i \quad (x_i < x \leq x_j), \end{aligned}\right\} \tag{2.8}$$

where the subscript j is used to denote the values of variables at the jump. The inlet value e_i is not known at this stage, but is such that $e_i > e_o$, by virtue of (2.3).

The proposed solution can be depicted on the swallowtail surface of Figure 1, the arrow there indicating the jump of the solution track at the discontinuity. It is easier to visualise the situation, however, by superimposing the two cross-sections $e = e_o$ and $e = e_i$ in the same diagram, as in Figure 4, where we have chosen $e_o = 1$ and $e_i = 0.85$ for demonstration purposes. The solution track is continuous and transfers from the supercritical branch of the $e = e_i$ section to the subcritical branch of the $e = e_o$ section where the massflow is Q_j. The change in slope of the track exhibits directly the known properties that $[u] < 0$ and therefore (as $[Q] = 0$) $[y] > 0$.

It remains to set the specific energy level e_i, but before this matter can be addressed we need to establish a property which has been tacitly assumed. We are supposing that, for the given outlet values, the channel is too long to support a continuous flow and we need to show that a discontinuous flow of the type sought is possible over the longer channel.

Reference to (2.4) and Figure 4 shows that u increases with e, at

each Q. Therefore y decreases as e increases, at each Q, and so does $y - s$. From the discharge law $Q' = -f(y-s)$ it now follows that $|Q'|$ decreases as e increases. Since $Q(x_o) = Q_o$ is fixed and $Q' \leq 0$, we deduce that at each $x < x_o$, $Q(x)$ decreases as e increases. Therefore the channel length $x_i - x_o$ increases with e for a fixed interval $Q_o \leq Q \leq Q_i$. Put the other way round, the interval $[Q_o, Q_i]$ decreases as e increases, if the channel length is fixed. The implied relaxation of the constraint on the channel length is further enhanced by the fact that the limiting massflow $Q_c(e) = g^{1/2}(2e/3)^{3/2}$ increases with e, and so therefore does the maximum value of $Q_i - Q_o$. The desired result is now established, that a longer channel is possible if a flow takes place wholly, or partly, at a higher specific energy level.

A lower bound for e_i is supplied by the inequality

$$Q_i \leq Q_c(e_i), \tag{2.9}$$

which is necessary for the supercritical inlet flow to exist. The smallest value of e_i consistent with (2.9) corresponds to critical inlet flow and minimum energy loss at the jump. From Figure 4 and earlier observations about the swallowtail cross-section, taken in conjunction with the fact that $Q(x)$ is non-increasing, we infer that the location of x_j is uniquely fixed by e_i and moves towards the outlet as e_i increases. An upper bound on e_i thus emerges and it can be shown (see section 3) that for $Q_j \geq Q_o$ (and hence $x_j \leq x_o$) we require

$$e_i \leq y_o \left\{ \left(1 + 8F_o^2\right)^{3/2} + 1 - 4F_o^2 \right\} / 16F_o^2, \tag{2.10}$$

where the outlet Froude number $F_o \in (0,1)$, equality locating the hydraulic jump at outlet.

The restriction (2.10) in turn limits the length of channels over which discontinuous flows are possible, because of the need to satisfy (2.9). As in the case of continuous flows, this limitation need not apply if part of the flow is at, or below, the level s, for that part of the flow is uniform and can be of arbitrary extent. Now the maximum depth available to the incoming supercritical flow is $y_c(e_i) = 2e_i/3$. Recalling that discontinuous solutions are sought in the case $s < 2e_o/3 < 2e_i/3$, we see that the incoming flow level may be above, at, or below the level s. The inlet depth $2e_i/3$ for minimum $[e]$ is above this level. Evidently, there are several possible configurations for the discontinuous flow. The water level may be wholly above the control level s, or the incoming flow may be uniform and below or at that level. In the latter case there is the further possibility of a three part flow consisting of supercritical flow above the level s at inlet and falling to that level, a uniform supercritical flow at level s (and of arbitrary length) and a jump connecting this uniform flow to the subcritical flow, which rises to depth y_o at outlet.

Clearly, a discontinuous flow is also possible in the case $F_o < 1, 2e_o/3 < s$ whether or not a continuous flow can exist. A discontinuous flow is the only solution available if the subcritical outgoing flow is terminated by $Q = Q_s$ within the channel and in this case the incoming supercritical flow is uniform and below the sill. Note that in all cases involving a hydraulic jump we

necessarily have $F_i \geq 1$.

2.2 Sloping Bed

Wherever (2.2) applies, we have $e = \text{constant} - b(x)$, and therefore, for a wholly continuous flow, $e = e(x)$, where

$$e(x) = e_o + b(x_o) - b(x) \quad (x_i \leq x \leq x_o) \tag{2.11}$$

satisfies the outflow condition $e(x_o) = e_o$. It is consistent with applications to assume that $b(x)$ is a decreasing function of x, and therefore $e(x)$ is an increasing function of x. Further, since $Q(x)$ is a non-increasing function of x we infer that solution tracks, if they exist, lie entirely on the upper surface or entirely on the lower surface of the swallowtail. These tracks are no longer plane curves, but the fact that e varies with x in a prescribed way means that the overall features deduced for a horizontal bed remain intact.

For instance, the necessary condition (2.6) for a continuous flow to exist is amended to

$$Q_i \leq Q_c(e_i) \tag{2.12}$$

where the inlet specific energy level is given by $e_i = e_o + b(x_o) - b(x_i)$. Since $e_i < e_o$, (2.12) may appear to be a more stringent condition than (2.6), but this need not be the case as $Q(x)$ is modified by (2.11).

Other, similar, amendments to the earlier analysis follow, for continuous and discontinuous flows, by using local values of e and the control level s where appropriate. The control level $s(x)$ can be set arbitrarily and it need not be a fixed distance above the bed.

3 Exact Solutions for Horizontal Channels

The choice of a particular discharge law allows $Q(x)$ to be calculated, in principle. This function relates position on a solution track, in the sense of section 2, to physical position in the channel and determines, for that discharge law, whether each of the flows identified earlier can be realised.

It is a good deal easier to seek $y(x)$, rather than $Q(x)$, the two being related by (2.1), which implies that

$$Q = y\sqrt{2g\,(e-y)}. \tag{3.1}$$

Therefore

$$Q\prime = \frac{\{(2e-3y)\,y\prime + ye\prime\}}{\{2g\,(e-y)\}^{1/2}}, \tag{3.2}$$

which is a version of (1.1), and for a side-weir, reference to (1.3), (1.4) and (1.5) implies that

$$(2e-3y)\,y\prime + ye\prime = -2c\,(e-y)^{1/2}\,(y-s)^{3/2} \qquad (y>s). \tag{3.3}$$

Since $e(x)$ can be regarded as known, (3.3) determines $y(x)$ and $Q(x)$ is recovered from (3.2).

Chow [2] observed that (3.3) can be solved exactly for a horizontal channel, in which case $e\prime = 0$ and, with $e = e_o$,

$$y\prime = \frac{-2c\,(e_o - y)^{1/2}\,(y - s)^{3/2}}{(2e_o - 3y)} \qquad (y > s). \tag{3.4}$$

We have excluded critical flows here to ensure that $2e_o \neq 3y$. Integration of (3.4) is elementary, yielding

$$cx = -\frac{(3s - 2e_o)}{e_o - s}\left(\frac{e_o - y}{y - s}\right)^{1/2} - 3\sin^{-1}\left(\frac{e_o - y}{e_o - s}\right)^{1/2} + \text{constant} \qquad (y > s). \tag{3.5}$$

We choose $\sin^{-1} : (0, 1] \longrightarrow (0, \pi/2]$.

It is instructive to consider the special case $s = 3e_o/2$, for which only the subcritical flow is given by (3.5) (the supercritical flow is wholly below the sill). We find from (3.5) that

$$\left.\begin{aligned} y(x) &= e_o\left\{1 - \tfrac{1}{3}\sin^2\tfrac{c}{3}\,(\gamma - x)\right\} \\ \gamma &= x_o + \tfrac{3}{2}\sin^{-1} 3\left(1 - \tfrac{y_o}{e_o}\right) \end{aligned}\right\}, \tag{3.6}$$

which satisfies $y(x_o) = y_o$ and holds for $x_o \geq x \geq \alpha - 3\pi/2c$. The corresponding massflow $Q(x)$ follows from (3.1) with $e = e_o$. The maximum weir length, L, which can support a continuous flow with depth profile (3.6) is

$$L = \frac{3\pi}{2c} - \frac{3}{c}\sin^{-1} 3\left(1 - \frac{y_o}{e_o}\right),$$

this flow being critical at the inlet. Note that $y(x_i) = s$ and hence that $y\prime(x_i) = 0$, so that we can smoothly join onto (3.6) a critical flow of arbitrary length at sill level. This is an example of the type of two part flow mentioned after (2.7).

For values of $s \neq 2e_o/3$, the mapping (3.5) must be inverted numerically. We can still infer some properties of the solution, however, without having $y(x)$ explicitly available. From (3.4) and (3.5) we see that, for a subcritical flow with $s > 2e_o/3$, $y\prime \to 0_+$ and $x \to -\infty$ as $y \to s_+$. Thus Q cannot attain the value Q_s in a finite distance and the side-weir can have unlimited length in this case. The two part solution is therefore only possible for $s = 2e_o/3$. Similarly, with $s < 2e_o/3$, an incoming supercritical flow can only attain the sill level asymptotically, ruling out, for the side-weir, the three part flow mentioned at the end of section 2.

In contrast to this situation, if the discharge law (1.7) is used in place of (1.5), then

$$y\prime = \frac{-2\epsilon cB(y-s)^{\frac{1}{2}}(e_o - y)^{\frac{1}{2}}}{2e_o - 3y}$$

and

$$\epsilon cBx = \frac{1}{2}(e_o - 3s)\sin^{-1}\left(\frac{e_o - y}{e_o - s}\right)^{\frac{1}{2}} - \frac{3}{2}(y-s)^{\frac{1}{2}}(e_o - y)^{\frac{1}{2}} + \quad \text{constant}$$

replace (3.4) and (3.5) respectively. These show that the free surface meets the

control level s smoothly within a finite distance of the outlet for an outgoing subcritical flow and within a finite distance of the inlet for an incoming supercritical flow. While this illustrates the sensitivity of the flows to the discharge law, it is somewhat theoretical if (1.7) is being used to model the discharge due to a rack, where $s = 0$.

Returning to the side-weir case, it is possible to investigate the curvature y'' of the free surface by using (3.4). The calculation is straightforward and its outcome is presented in Figure 5 which shows how the curvature changes with the dimensionless depth y/e_o and the dimensionless sill height s/e_o. There is a narrow sill height band $(4\sqrt{3} - 5 < 3s/e_o < 2)$ in which the curvature of a subcritical flow can change twice.

We recall that, if $s < 2e_o/3$, the channel length which can support both sub- and supercritical continuous flow is determined by $Q = Q_c$. Using this condition in the form $y = y_c = 2e_o/3$ in (3.5) we find that the maximum channel length for the outlet values $y = y_o, e = e_o$ is given by

$$cL_{\max} = 3\sin^{-1}\left(\frac{e_o}{3(e_o - s)}\right)^{\frac{1}{2}} + 3\sin^{-1}\left(\frac{e_o - y_o}{e_o - s}\right)^{\frac{1}{2}}$$

$$- (e_o - s)^{-1}(2e_o - 3s)^{\frac{1}{2}}\left\{\sqrt{e_o} + \sqrt{\frac{(2e_o - 3s)(e_o - y_o)}{y_o - s}}\right\}.$$

This relationship is shown in Figure 6 as a function of y_o/e_0, for the value $s/e_o = 0.4$, forming the inner boundary of the regions in which continuous flow is possible. The lower branch of this boundary tends to the value s/e_o

as $L_{\max} \longrightarrow \infty$, as we have already established. It can be shown that the value of $L_{\max}$, as given above, increases with s/e_o for each $y_o/e_o \neq 2/3$.

For discontinuous flows, the backwater analysis requires the relationship

$$y_- = \frac{y_+}{2}\left\{\left(1+8F_+^2\right)^{\frac{1}{2}} - 1\right\}, \tag{3.7}$$

which is derived from (2.8); the subscript notation was given in section 1.

If the jump location x_j is prescribed, y_+ is given by inverting (3.5), the constant in that equation having been determined by $y_o = y(x_o)$. Since $F_+^2 = 2(e_o - y_+)/y_+$, y_- is readily found from (3.7) and u_- and $e_- = e_i$ follow by using (2.1) and (2.8). Alternatively, $e_i = e_o - [y]^3/4y_+y_-$, as may be deduced from Stoker [9] or from (2.8). Replacing e_o by by e_i in (3.5) and fixing the constant afresh by $y(x_j) = y_-$, we can deduce $y(x)$ by inversion for the supercritical flow upstream of the jump. In practice, an iterative process based on the discontinuous flow calculation described is usually necessary to meet the flow condition $Q_i \leq Q_c(2e_i/3)$ if the total weir length is assigned in advance.

Further detail can be added to the general structure deduced in section 2. For instance, we can determine the longest side-weir which can support a discontinuous flow, in the case (2.7)(b). It follows from the previous section that the maximum weir length occurs with the jump located at x_o. Therefore, from (3.7),

$$y_- = \frac{1}{2} y_o \left\{ \left(1 + 8F_o^2\right)^{\frac{1}{2}} - 1 \right\}$$

and using this value together with $Q_- = Q_o$, we find that the specific energy of the corresponding incoming flow is

$$e_i = e_- = y_o \left\{ \left(1 + 8F_o^2\right)^{\frac{3}{2}} + 1 - 4F_o^2 \right\} / 16F_o^2,$$

a value quoted in (2.10).

If $y_- > s$, the supercritical flow is wholly above the sill and the required maximum length is therefore the maximum length of the continuous supercritical flow with $y = y_-$ and $e = e_i$ at outlet. This length is given by the existing expression for $L_{\max}$ with y_- replacing y_o and e_i replacing e_o. If $y_- \leq s$, the incoming flow is uniform and of unlimited length.

The curve representing maximum side-weir length for a discontinuous flow is plotted on Figure 6, completing our illustration of that classification diagram for $s < 2e_o/3$. It forms the boundary, in the subcritical regime, between the region in which discontinuous flows are possible and the region in which no flows are possible. As $L_{\max} \longrightarrow \infty$, the curve tends to the level

$$\frac{y_o}{e_o} = \frac{1}{8} \left\{ 4 - \frac{s}{e_o} + \sqrt{16 - \frac{8s}{e_o} - 15\left(\frac{s}{e_o}\right)^2} \right\}$$

from below; this level corresponds to $y_- = s$. The value of $L_{\max}$ increases with s/e_o for each $y_o/e_o > 2/3$, and the upper and lower boundaries of the no-flow region both degenerate to the straight line $y_o = 2e_o/3$ as $s \longrightarrow 2e_o/3$ from below.

The corresponding diagram for any $s \geq 2e_o/3$ is trivial as all flows have unlimited length; we have shown, in particular, that $s = 2e_o/3$ gives a two part flow.

Figures 7—9 give sample results of the free surface elevation obtained by using a bisection algorithm to invert (3.5). The three test problems all consist of a 5m channel that is 1m wide. The sill height is 0.5m and the weir coefficient, c, is 0.9. Outflow depth is taken to be 0.7m, that is, 20cm above the sill height. The three problems can now be distinguished by just specifying the massflow at outlet. For the first (subcritical) problem we take $Q = 0.01m^3s^{-1}$, for the second, supercritical, case we take $Q = 6.0m^3s^{-1}$ and finally for the transcritical case $Q = 1.0m^3s^{-1}$, for which the incoming flow is at sill level. The exact solutions to problems 1,2 and 3 are shown in Figures 7,8 and 9 respectively The predicted curvature and maximum weir lengths have been confirmed for a wide range of the parameters.

The equation (3.3) is analytically intractable for non-horizontal channels and the numerical solution method described next is required to add quantitative detail to the flows deduced in section 2. The development given here acts as a useful guide, of course, to the purely numerical solutions.

4 Numerical Solutions

For the purpose of obtaining numerical solutions, it has been traditional to write Ordinary Differential Equations (ODEs) in the form

$$y' = f(x, y) \tag{4.1}$$

where x is the independent variable and $y(x)$ is to be found. Solution techniques for this type of equation are well-known and well-documented, see Henrici [5] or Lambert [6] for example. Rather less well-known (see Fox & Mayers [3]) are solution techniques that deal with equations of the form

$$G(x, y, y') = 0 \tag{4.2}$$

$$\text{or} \qquad y' = g(x, y, y'). \tag{4.3}$$

We will refer to these solution techniques as Implicit Differential Equation Solvers, or IDES for short. Equations in the form (4.1) have obvious advantages, but there may be situations where it is preferable to use the form represented in (4.3). The obvious case is when the function, G in (4.2), is just not separable due to nonlinearity in the term y'.

For our particular application the steady state equation (for depth) is in the form (1.1). This form is not atypical, in shallow water theory, despite the novel application. Problems arise, though, in computations if the Froude number, F, passes through unity, that is the flow changes from subcritical flow to supercritical flow, or indeed if F just gets sufficiently close to 1, as in these cases the right hand side of (1.1) becomes unbounded for computational purposes, with $\alpha = 1$. The division by the factor $1 - F^2$, or $1 - \alpha F^2$ more generally, is rather

artificial and the equation naturally appears as momentum balance in the form

$$y\prime = \alpha F^2 y\prime + S_0 - S_f - \frac{\alpha Q Q\prime}{gA^2}. \tag{4.4}$$

(In this section we will return to the more usual notation, in hydraulics literature, of using Q to represent the total massflow in the channel. However, since we shall be taking $B = 1$ in the test cases $Q \equiv \tilde{Q}$.) The division by $1 - \alpha F^2$ is just performed to get the equation into the form of (4.1).

The shallow water equations were first solved in the form (4.4) by Chawdhary [1] and also appeared in Samuels & Chawdhary [7], although they were not concerned with discharge flows, Q being constant. We shall give details of the algorithm and will show that the method is capable of giving accurate results for backwater analyses of both subcritical and supercritical flows. The results in [1] and [7] indicate that the method also deals with the transcritical case. Certainly their work shows that the method does not fail as the critical point is reached but we argue that in the cases considered here another boundary condition is required to give the problem a unique solution. (It is possible that the transcritical case was successfully solved in [1] because the jumps were forced by changes in the bed-slope). The important point, though, is that IDES are capable of solving sub- and supercritical backwater problems and will not blow up as a critical point is approached.

We discretize the equations at certain, not necessarily equi-spaced, points x_n. The distance between x_n and x_{n+1} is denoted by $\Delta x_{n+\frac{1}{2}}$, which, with-

out loss of generality, will be assumed to take a constant value Δx in this work. The approximate solution at these points is then denoted by y^n. As we are solely concerned with backwater analyses in this paper we will therefore assume that y^{n+1} is known and y^n is to be found. To find y^n we perform an iteration on this value and we will denote the k^{th} approximation to y^n simply by y^k, the value of n being understood. The bed-slope, S_0, will be a constant for our calculations here, but this is not a restriction of the method (see [1]). Following Chawdhary [1] equation (1.1) is now discretised, using the trapezium rule, in the form

$$\begin{aligned}\frac{y^{n+1}-y^{k+1}}{\Delta x} &= \frac{\alpha}{2}\left(F^{k^2}+F^{n+1^2}\right)\frac{y^{n+1}-y^k}{\Delta x}+S_0-\frac{1}{2}(S_f^k+S_f^{n+1}) \\ &- \frac{\alpha}{2g}\left(\left.\frac{QQ\prime}{A^2}\right|^{n+1}+\left.\frac{QQ\prime}{A^2}\right|^{k}\right). \qquad (4.5)\end{aligned}$$

With a little re-arrangement the scheme then becomes,

$$y^0 = y^{n+1}$$

$$\begin{aligned}y^{k+1} &= y^{n+1}+\frac{\alpha\Delta x}{2g}\left(\left.\frac{QQ\prime}{A^2}\right|^{n+1}+\left.\frac{QQ\prime}{A^2}\right|^{k}\right)-\frac{\alpha}{2}\left(F^{k^2}+F^{n+1^2}\right)\left(y^{n+1}-y^k\right) \\ &\quad -\Delta x S_0+\frac{\Delta x}{2}\left(S_f^k+S_f^{n+1}\right) \quad \text{for} \quad k=0,1,2,... \qquad (4.6)\end{aligned}$$

The condition that ensures the iteration (4.6) converges is simply that

$$\left|\frac{\partial y^{k+1}}{\partial y^k}\right| < 1. \qquad (4.7)$$

In principle we could check (4.7) exactly for the iteration (4.6), but this would be cumbersome. However, the terms we might wish to avoid are all multiplied

by Δx. Hence they can be made as small as we wish (if $y \neq 0$) by control of the space step Δx. We shall argue later that it is beneficial for other reasons to use what computational time is available solving on a finer mesh, rather than using the same time on a more complex iterative scheme with a coarser mesh. The term we cannot control in this fashion is the one involving the Froude number. Hence for supercritical flow, or more generally when $\alpha F^2 > 1$, we re-arrange (1.1) as

$$y\prime = \frac{1}{\alpha F^2}\left(y\prime + \frac{\alpha Q Q\prime}{gA^2} - S_0 + S_f\right).$$

This equation can then be discretised in the same manner as (4.6). The Froude number is a quantity that will need to be calculated anyway and so this approach results in little extra computational cost. If, as is likely in practice, we are unable to substitute for Q from equation (2.1) and have to solve (1.1) together with (1.10) as a system then the condition (4.7) is replaced by a constraint on the norm of the equivalent Jacobian matrix. We have never found a situation where the extra cost of this approach was justified over the much simpler Froude number condition.

First we apply our scheme to the one-equation model, (3.4), where Q and $Q\prime$ have been substituted for. The three problems discussed earlier, whose analytic solutions are shown in Figures 7—9, were solved by the numerical approach and the solutions are shown in Figures 10—12 for 64 grid points. A summary of the results from running the scheme on various meshes can be seen in Tables i—iii, giving the error in inlet values. All these results were obtained using a large number, 256, of iterations to try and eliminate this source of error.

We see that for the smooth solutions second order accuracy is achieved, whilst in the discontinuous case the scheme reduces to first order as we would expect from approximation theory. Generally speaking, more points are therefore needed to resolve this case. In the case of transcritical flow an iterative procedure was used, as alluded to in the previous section, to find the smallest jump giving a physical inlet value. The numerical backwater analysis, for this case, involves calculating a subcritical flow from outlet until the critical depth is reached. A jump must then be fitted from the subcritical solution and we try to reach inlet with the resulting supercritical flow. If this fails we position progressively stronger jumps nearer the outlet until a supercritical flow results that can reach inlet. If this is achieved, any jump nearer outlet will also produce a physical flow; an inlet boundary condition, like the one given above for example, selects a unique solution in this case. No flow exists if the jump reaches the outlet before such a supercritical flow is found.

We now look at the convergence rate of the iteration. For this we consider the harder of the two continuous problems, Problem 2, with 64 points and varying numbers of iterations. Table iv shows the errors and convergence of the sequence of solutions. From these results it is very difficult to give any firm conclusions as to the order of the iteration. It does, however, seem to start as a low order convergence and then rapidly accelerates as the exact answer is approached. The precise nature of the convergence of this iteration is the subject of further work.

We have established in numerous numerical experiments that the

IDES technique can solve side-weir problems governed by (3.4) for all flow regimes. Of course, the real point of a numerical method is to be able to solve problems that cannot successfully be treated analytically, in particular, because a non-zero friction implies that the energy is not known. This means that we will need to solve equations (1.1) and (1.3) as a system . Equation (1.1) is discretised as before. At the same time we discretise (1.3) using the trapezium rule with the implicit terms on the right-hand side again lagged, that is, using the previous iteration value, to give an explicit expression for the new value Q^{k+1}. We update from (1.3) first and then use the latest value of Q^{k+1} to update y^{k+1} from the discretisation of (1.1). This choice seems to have no effect on the scheme. To validate this approach Problem 2 is again solved but this time with the two-equation model, that is without assuming constant energy. Errors, arranged as before, are shown in Table v. The order of the scheme is again definitely shown to be 2. Comparing with the results in Table ii we see that the errors are very comparable, being slightly better for the depth and slightly worse for the massflow. Although it does not show up clearly in plots of the solution, as the error is very small, the energy is no longer constant, as we would expect since this property is no longer enforced. Also, we are not able to calculate a solution on some of the coarser meshes.

We have also successfully solved problems with tapering, sloping channels, with friction and with values of $\alpha \neq 1$. It has also been reported to us by Wixcey [10], that, using the same technique as presented here, similar problems have been solved in channels of non-rectangular cross-sections.

5 Acknowledgment

The authors wish to thank Drs. John Wixcey and Roland Price of HR Wallingford, who inspired this work by drawing our attention to some of the problems arising from flow in side-weirs and who supplied valuable background information.

References

[1] Chawdhary, K.S., *"On the Solution of Implicit First-Order Differential Equations."* M.Sc. Dissertation, Dept. of Mathematics, University of Reading, 1991.

[2] Chow, V.T., *"Open-Channel Hydraulics."* McGraw Hill, 1959.

[3] Fox, L. & Mayers, D.F., *"On the Numerical Solution of Implicit Ordinary Differential Equations."* IMA J. Numer. Anal., **1**, pp. 377-401, 1981.

[4] Henderson, F.M., *"Open Channel Flow."* MacMillan, 1966.

[5] Henrici, P., *"Discrete Variable Methods in Ordinary Differential Equations."* John Wiley & Sons, 1962.

[6] Lambert, J.D., *"Computational Methods in Ordinary Differential Equations."* John Wiley & Sons, 1973.

[7] Samuels, P.G. & Chawdhary, K.S., *"A Backwater Method for Trans-Critical Flows."* 2^{nd} Int. Conf. on Hydraulic & Environmental Modelling of Coastal, Estuarine and River Waters, University of Bradford, 22-24 September 1992.

[8] Sewell, M.J. and Porter, D., *"Constitutive surfaces in fluid mechanics."* Math. Proc. Camb. Phil. Soc., **88**, 1980.

[9] Stoker, J.J., *"Water Waves: The Mathematical Theory with Applications."* Interscience Publishers, 1957.

[10] Wixcey, J.R., *Private Communication*, Wallingford Software, HR Wallingford Ltd., Oxfordshire, 1992.

List of Figures

List of Tables

No. of points	Error in depth	Error in massflow	Order of convergence
1	0.076134	0.153676	—
2	0.020284	0.026666	1.91
4	3.634×10^{-3}	4.146×10^{-3}	2.48
8	8.358×10^{-4}	9.308×10^{-4}	2.12
16	2.053×10^{-4}	2.28×10^{-4}	2.03
32	5.1×10^{-5}	5.66×10^{-5}	2.01
64	1.2×10^{-5}	1.41×10^{-5}	2.09
128	3×10^{-6}	3.5×10^{-6}	2.0
256	1×10^{-6}	1×10^{-6}	1.58

Table i: Errors for Problem 1 using the one equation model.

No. of points	Error in depth	Error in massflow	Order of convergence
1	Iteration	diverged	—
2	0.216205	0.792889	—
4	0.536265	1.17698	—
8	0.69783	1.27619	—
16	0.096055	0.297298	2.86
32	0.02091	0.06769	2.19
64	5.08×10^{-3}	0.016597	2.04
128	1.264×10^{-3}	4.13×10^{-3}	2.0
256	3.17×10^{-4}	1.032×10^{-3}	2.0

Table ii: Errors for Problem 2 using the one equation model.

No. of points	Error in depth	Error in massflow	Order of convergence
1	0.2063866	0.22127	—
2	0.2063866	0.22127	—
4	0.2063866	0.22127	—
8	0.0806906	0.056772	1.35
16	0.021496	0.010409	1.91
32	0.02067343	9.9405×10^{-3}	0.06
64	6.416×10^{-3}	2.6934×10^{-3}	1.69
128	6.3536×10^{-3}	2.666×10^{-3}	0.01
256	2.75×10^{-3}	1.1134×10^{-3}	1.21

Table iii: Errors for Problem 3 using the one equation model.

No. of iterations	Error in depth	Error in massflow	Order of convergence
1	1.133698	5.797245	—
2	0.737708	3.3309832	0.62
4	0.2793413	1.050197	1.40
8	0.050947	0.170757	2.45
16	3.626×10^{-3}	0.011833	3.81
32	4.2×10^{-5}	1.35×10^{-4}	6.43
64	0.0	0.0	—
128	0.0	0.0	—

Table iv: Errors for Problem 2 using the one equation model.

No. of points	Error in depth	Error in massflow	Order of convergence
8	0.3470903	1.694867	—
16	0.0610075	0.3181655	2.51
32	0.014248	0.076558	2.10
64	3.5011×10^{-3}	0.01904	2.02
128	8.72×10^{-4}	4.757×10^{-3}	2.01
256	2.18×10^{-4}	1.19×10^{-3}	2.00

Table v: Errors for Problem 2 using the two equation model.

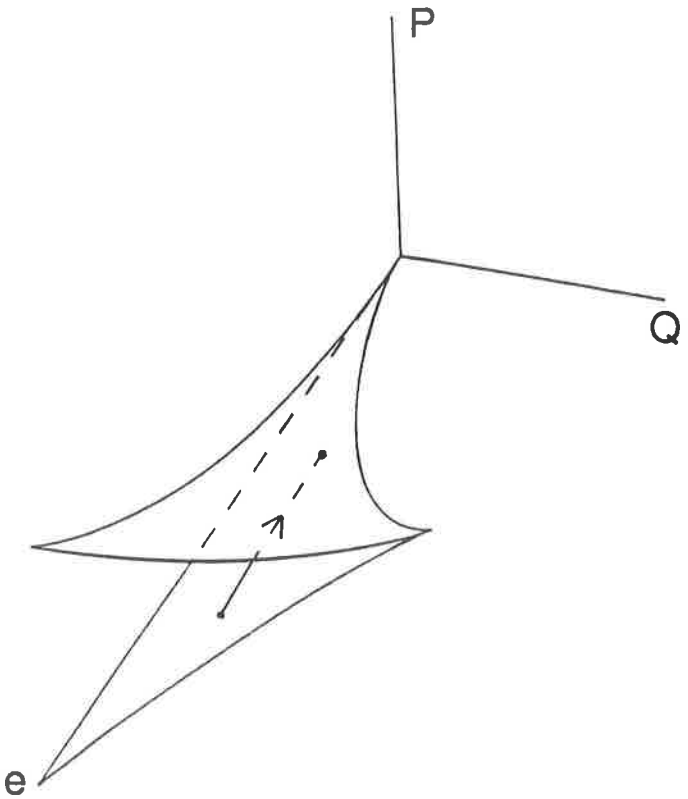

Figure 1: The surface $P = P(Q, e)$.

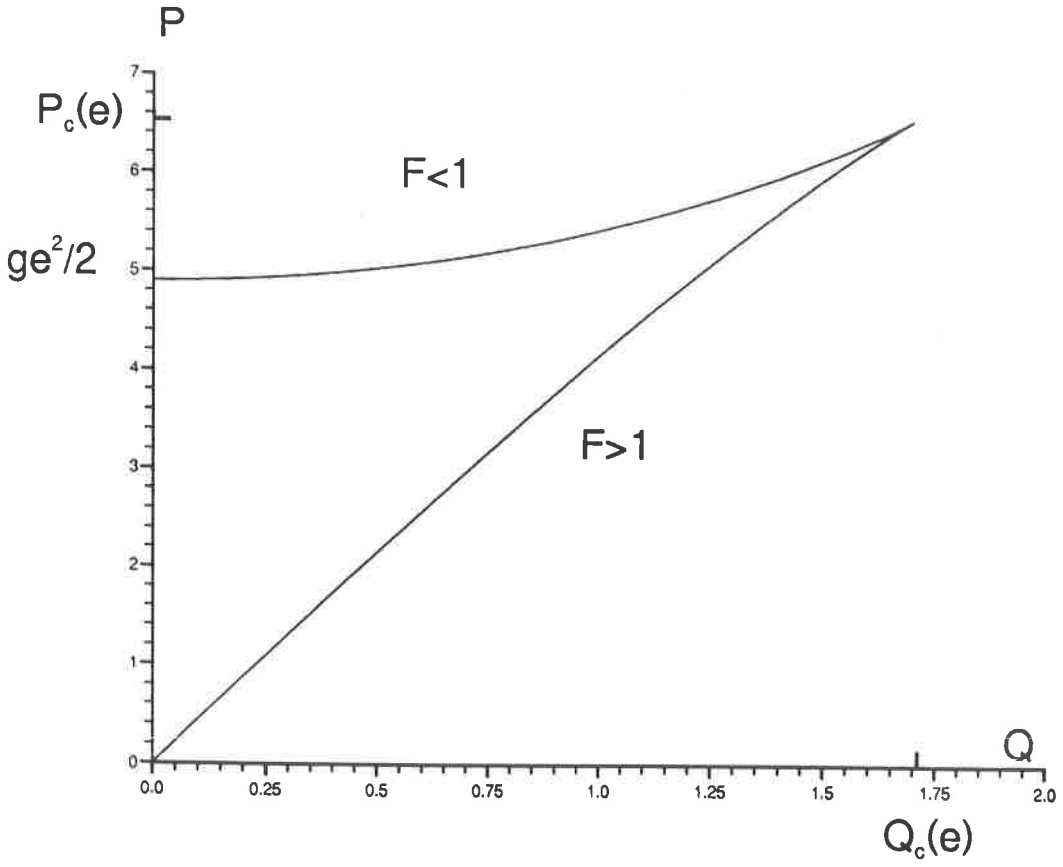

Figure 2: The cross-section $e = 1$ of $P = P(Q, e)$.

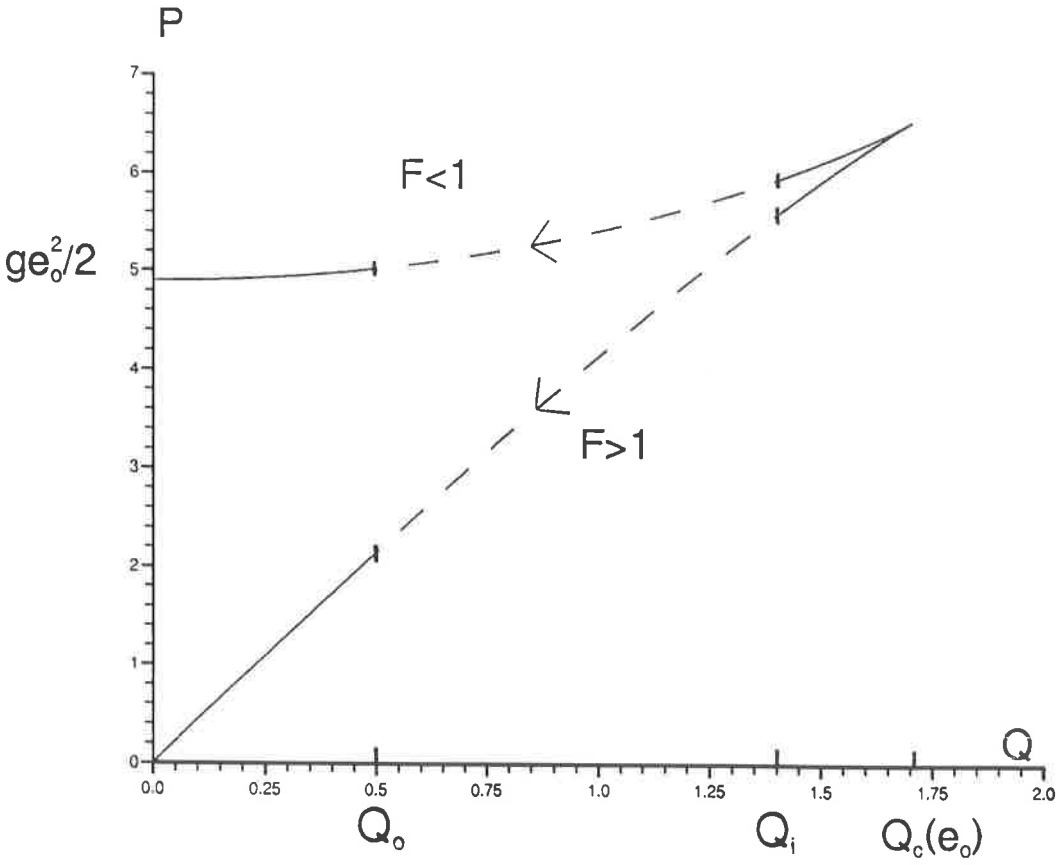

Figure 3: Solution tracks for continuous discharge flow over horizontal bed.

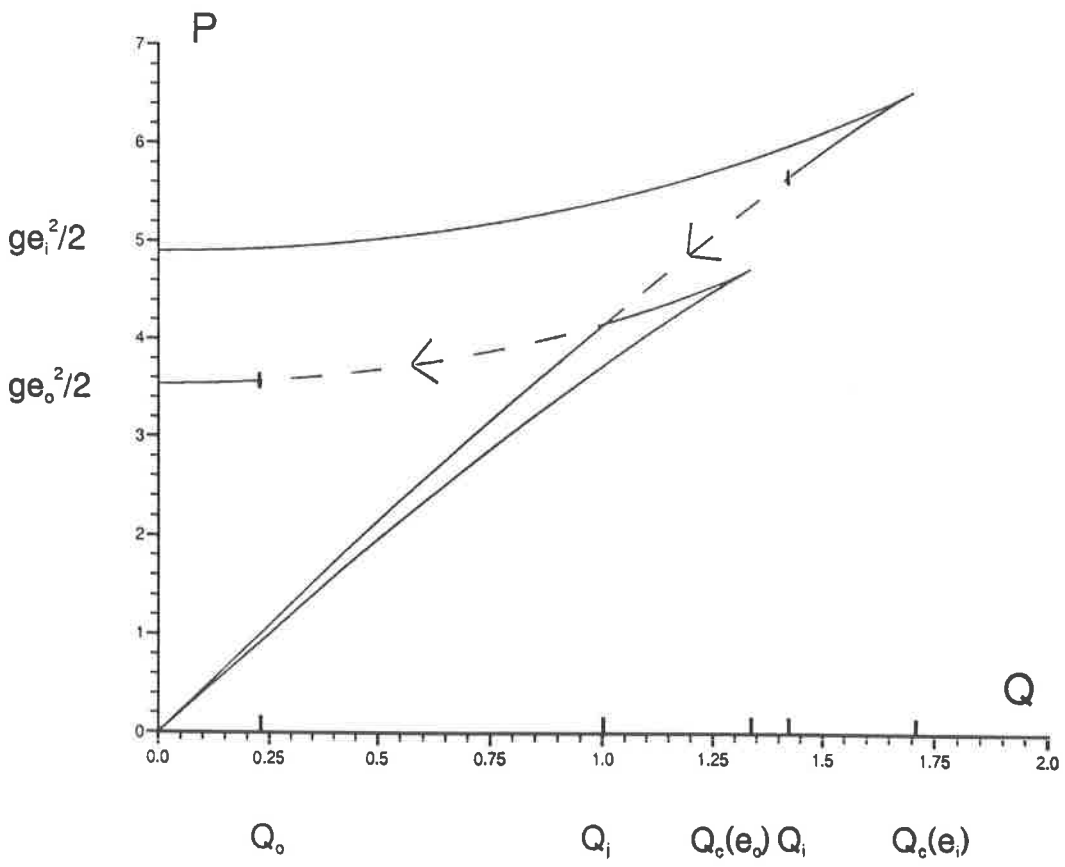

Figure 4: Solution track for discontinuous discharge flow over horizontal bed.

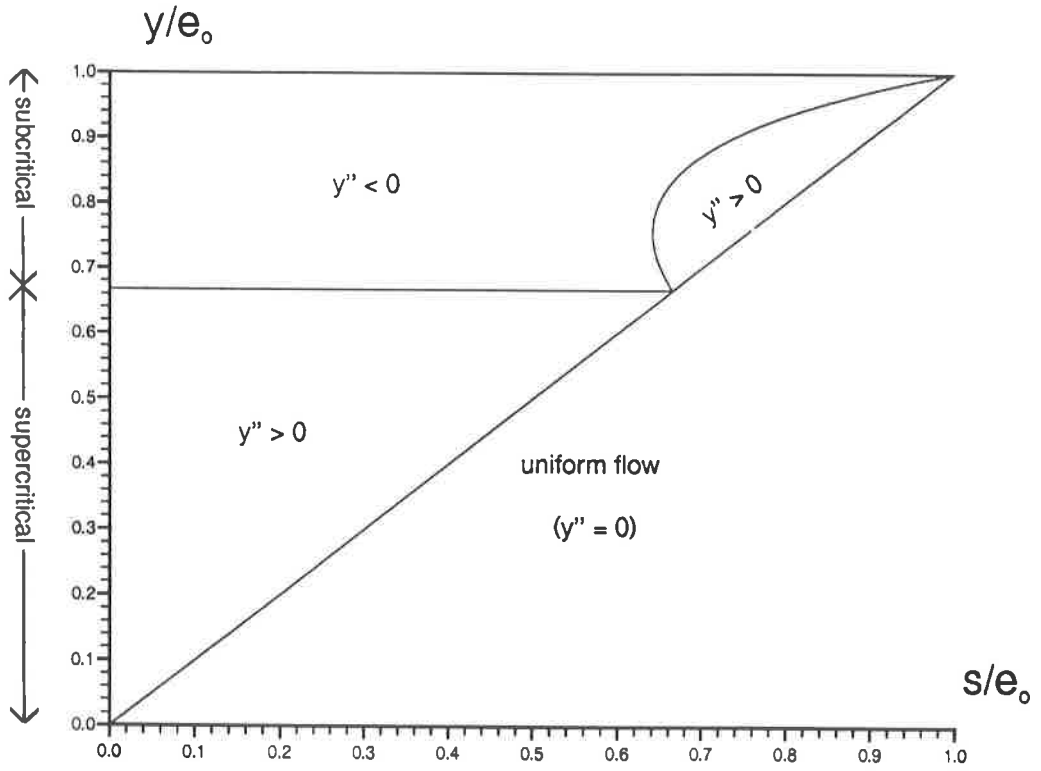

Figure 5: Free surface curvature for side-weir flow over horizontal bed. The curved region in the subcritical regime is bounded by segments of $y/e_o = \frac{1}{12}\left\{11 - 3\xi \pm (9\xi^2 + 30\xi - 23)^{1/2}\right\}$, where $\xi = s/e_o$.

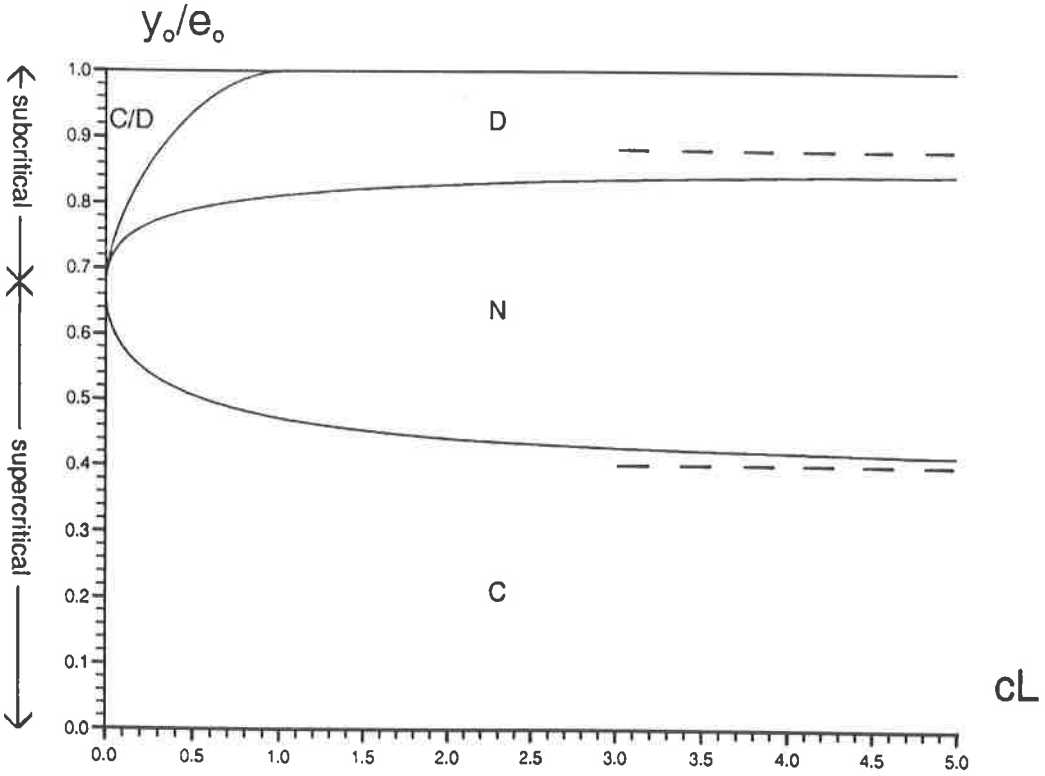

Figure 6: Classification diagram for side-weir, with $s/e_o = 0.4$: C—continuous flows possible; C/D—continuous or discontinuous flows possible; D—discontinuous flows possible; N—no flows possible. The boundaries of the regions are the curves $cL_{\max}$.

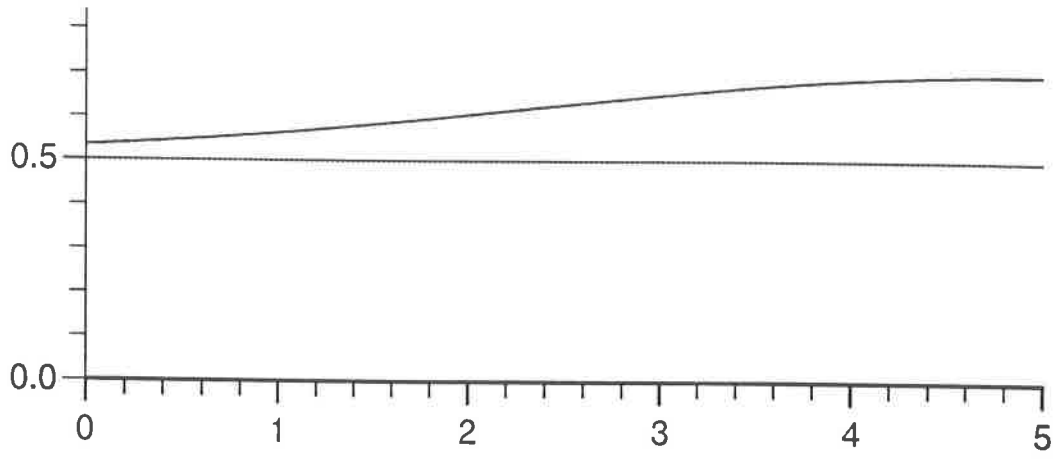

Figure 7: Water depth for side-weir: Problem 1. Inflow depth and massflow are 0.534426m and $0.962776 m^3 s^{-1}$.

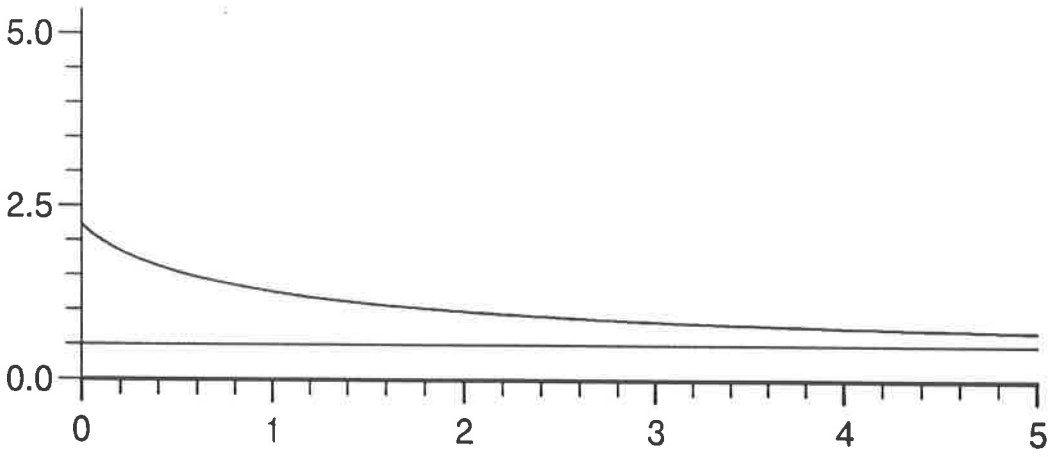

Figure 8: Water depth for side-weir: Problem 2. Inflow depth and massflow are 2.23097m and $14.7079 m^3 s^{-1}$.

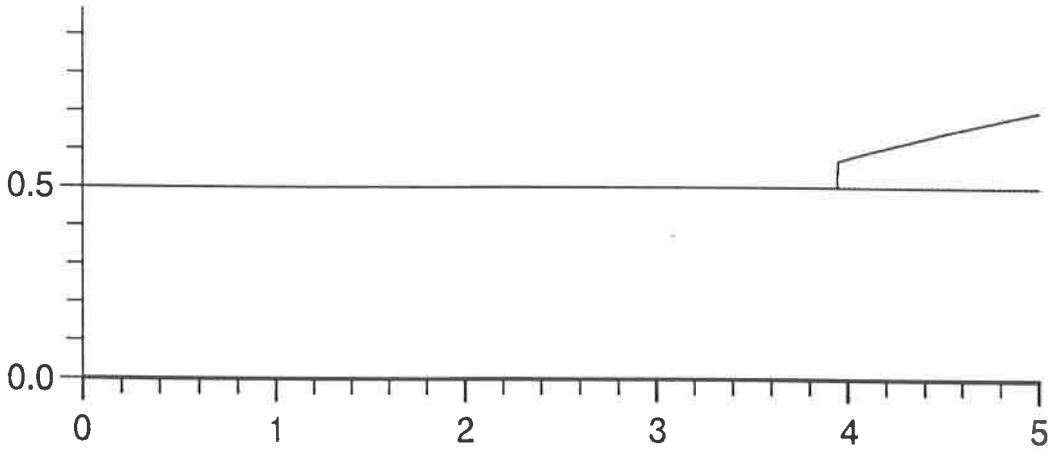

Figure 9: Water depth for side-weir: Problem 3. Inflow depth and massflow are 0.49985m and 1.22127$m^3 s^{-1}$. Froude no. is 1.2186.

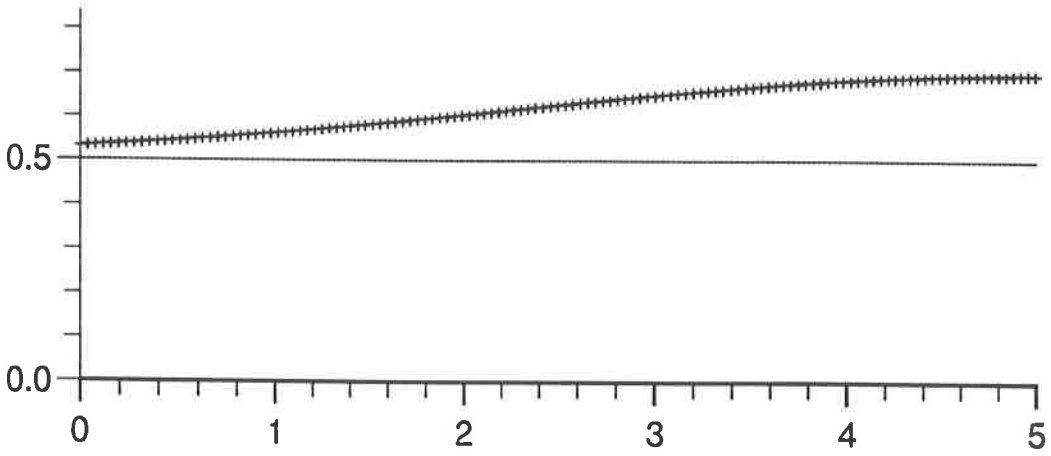

Figure 10: Water depth for side-weir: Problem 1 with 128 pts. Inflow depth and massflow are 0.534429m and $0.9627725 m^3 s^{-1}$.

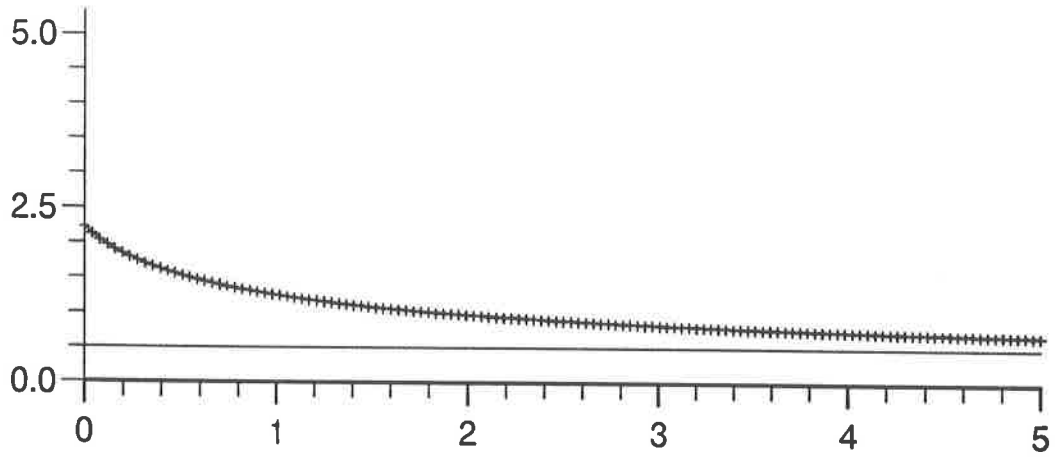

Figure 11: Water depth for side-weir: Problem 2 with 128 pts. Inflow depth and massflow are 2.232234m and $14.71203 m^3 s^{-1}$.

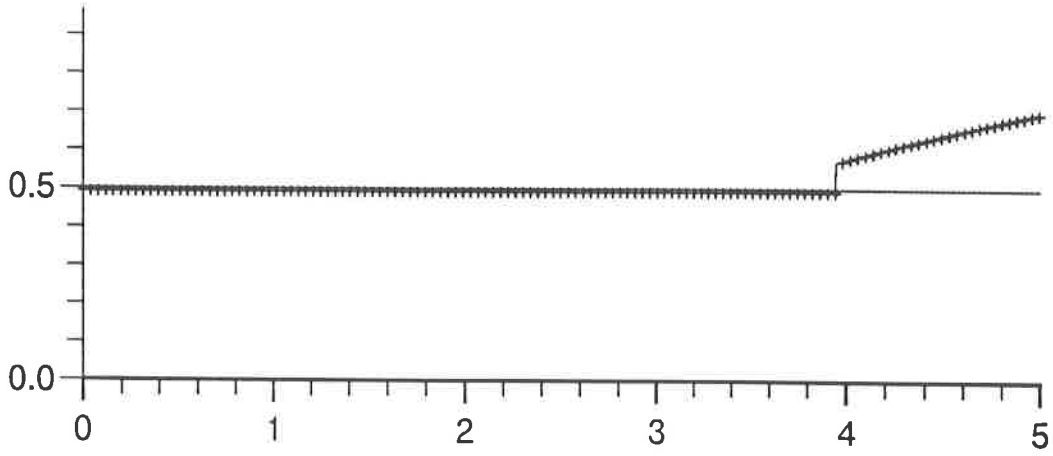

Figure 12: Water depth for side-weir: Problem 3 with 128 pts. Inflow depth and massflow are 0.4934964m and $1.218604 m^3 s^{-1}$.